# *In Situ* Fluorescence Spectroscopic Studies of Polymerization of Anaerobic Adhesives

**Eerik Maandi, Chong Sook P. Sung**

*Polymer Program, Department of Chemistry, Institute of Materials Science, University of Connecticut, Storrs, Connecticut 06269-3136*

Received 16 April 2007; accepted 5 October 2007
DOI 10.1002/app.27543
Published online 5 December 2007 in Wiley InterScience (www.interscience.wiley.com).

**ABSTRACT:** Anaerobic adhesives cured by a redox initiated free radical mechanism contain acrylate monomers, stabilizers, accelerators, a nonreactive fluorophore used as an inspection aid, and various nonreactive ingredients to modify polymer properties and rheology. Fluorescence spectroscopy has shown that collisional quenching of the fluorophore due to an amine cure-accelerator is reduced by rising viscosity during polymerization, thus resulting in an increase in fluorescence intensity. By monitoring the changes in fluorescence intensity with an *in situ* fiber-optic method, room temperature polymerizations have been characterized both in a model formulation containing only reactive ingredients as well as in a real commercial formulation containing many nonreactive ingredients. The results from this fluorescence method on polymerization monitoring show excellent correlation with the FTIR results. © 2007 Wiley Periodicals, Inc. J Appl Polym Sci 107: 3685–3693, 2008

**Key words:** fluorescence spectroscopy; polymerization monitoring; anaerobic adhesives; FTIR spectroscopy

## INTRODUCTION

Adhesives cured by a redox initiated free radical mechanism have been known in industry for over two decades.[1] A subset of this group is the acrylic anaerobic adhesives, which cure in the absence of oxygen and encompass a wide variety of industrial uses for machinery adhesives for locking and sealing.[2] To exclude oxygen, the bond gaps of these materials are very small, typically on the order of 50 μm (~ 2 mil). Typical formulations contain (meth)acrylic monomers, stabilizers, accelerators, a fluorescing thiophene derivative used as an inspection aid, and other ingredients to modify polymer properties and rheology. The cure mechanism is a convoluted array of oxidation and reduction reactions and efforts to succinctly describe the process are still being postulated.[3–6] Commercially, the reaction proceeds by the addition of a transition metal to an adhesive composition containing a peroxide as a free radical source. The transition metal may be in the form of a salt dissolved in solvent, or the substrate itself may be comprised of a transition metal (e.g., a nut and bolt). The latter condition has resulted in the development of the anaerobic adhesive industry which has grown steadily to its present value of approximately half a billion dollars in annual sales. As the oxidation/reduction process proceeds, the transition metal catalyzes peroxide decomposition to generate the free radicals necessary for chain initiation.[7] The general reaction scheme is shown in Scheme 1 where **m** represents the transition metal and **M** is the monomer.

When the peroxide is exposed to a transition metal capable of adjacent oxidation states, (Fe, Cu, V), the peroxide decomposes into an R-oxy radical and a hydroxyl radical that is immediately reduced to the anion while the metal is simultaneously oxidized in reaction (1). Reaction (2) shows the R-oxy radical reacting with monomer forming the active species for chain initiation. Reaction (3) shows the active monomer radical chain extending by reacting with another monomer during the propagation step. This process continues until either the monomer is consumed or until competing forces destroy the active centers by recombination or disproportionation as shown in reactions (4) and (5), respectively.

The conventional methods for *in situ* characterization such as fiber-optic fluorescence used for epoxy cure or UV reflection technique for monitoring imidization studies[8,9] is difficult to apply to anaerobic polymerization due to the unique requirements of this system including exclusion of oxygen through narrow bond gaps and the presence of a transition metal which typically involves the substrate to be bonded. By taking advantage of the presence of the fluorophore and working within the constraints of the system, a new *in situ* cure monitoring method has been developed and reported in this article.

*Correspondence to:* C. S. P. Sung (chong.sung@uconn.edu).
Contract grant sponsors: Henkel Corporation, B. J. and C. H. Park Foundation.

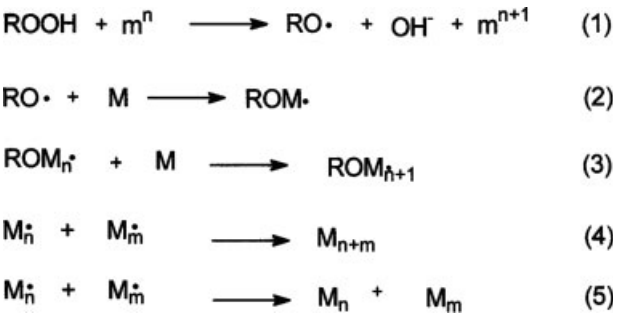


**Scheme 1** Proposed mechanism of anaerobic polymerization.[1–4]

## EXPERIMENTAL

UV spectra and the interaction of the individual ingredients were characterized using a Perkin–Elmer model Lamda 40P Spectrophotometer. Samples were dissolved in acetonitrile and evaluated using standard quartz cuvettes of both 1- and 10-mm-path length to obtain an analyte absorbance of less than one.

Cure studies were carried out by anaerobically polymerizing methacrylate monomers that have been formulated to contain the cure system components described in Table I. The chemical structures of the formulation are listed in Scheme 2. Experiments were performed at room temperature by placing the adhesive composition directly on a diamond ATR crystal used in a Perkin–Elmer Spectrum 2000 FTIR instrument and covering it with a steel lap shear. Real time data from infrared spectra was then analyzed to determine the extent of polymerization as a function of monomer concentration and time. The carbonyl peak from the ester of the methacrylate group at $\sim 1700$ cm$^{-1}$ is used as an internal standard since it does not change relative to the C—H bending peak at $\sim 810$ cm$^{-1}$ of the terminal carbon. As the polymerization reaction occurs, the intensity of the peak at 810 cm$^{-1}$ decreases. From the peak height information, the area ratio of C—H at $\sim 810$ cm$^{-1}$/C=O at $\sim 1700$ cm$^{-1}$ is then calculated for each scan and the percent of monomer conversion determined.

All fluorescence measurements were carried out using a Spectra Group Limited (Millbury, OH). CM-1000 Cure Monitor fitted with a bifurcated fused silica fiber-optic cable. The excitation source is a high-pressure xenon arc lamp. The detector is a 1024 × 64 pixel CCD capable of simultaneously collecting the entire emission spectrum. Similar to the UV–vis measurements, dilute solutions of analytes were analyzed using standard 1- and 10-mm-path length quartz curvettes. Because the fiber-optic cable carries both the excitation and emission information, the cable is placed at a 45° angle at a distance of 5 mm with respect to the sample to minimize the amount of excitation energy that is reflected back to the detector. For polymerization experiments, samples were placed between a quartz disc and a steel lap shear as illustrated in Scheme 3. Scheme 4 shows the setup of the fiber-optic fluorescence measurements.

**TABLE I**
**Composition of Model Anaerobic Formulation I**

| Ingredient | Weight % |
|---|---|
| HEMA | 96.955 |
| BS | 1.00 |
| DMpT | 1.00 |
| CHP | 1.00 |
| BBOT | 0.045 |

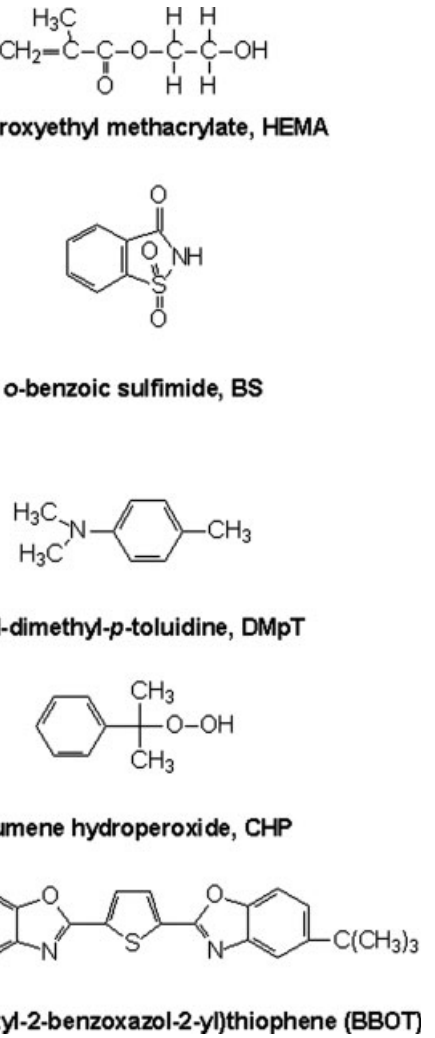


**Scheme 2** Chemical structures of the ingredients for model anaerobic formulation I.

## RESULTS AND DISCUSSION

The ingredients comprising anaerobic adhesive formulations have been analyzed by three techniques

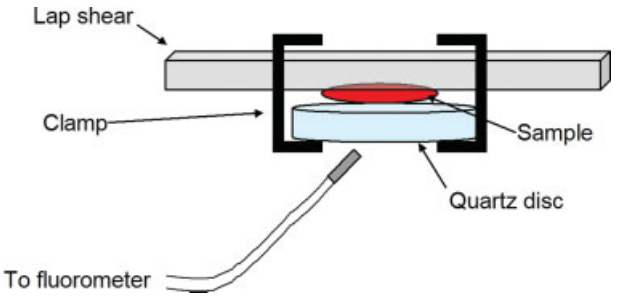


**Scheme 3** Fluorescence analysis of sample on quartz disc. [Color figure can be viewed in the online issue, which is available at www.interscience.wiley.com.]

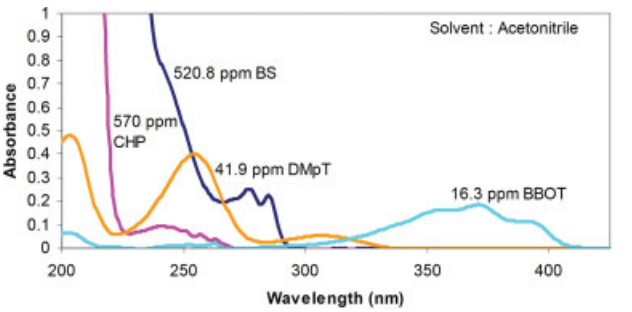


**Figure 1** UV spectra of additives used in anaerobic adhesive formulations. [Color figure can be viewed in the online issue, which is available at www.interscience.wiley.com.]

as described earlier; UV, fluorescence, and IR spectroscopy. The ingredients include the monomer, 2-hydroxy ethyl methacrylate (HEMA), two accelerators; *N*,*N*-dimethyl-*p*-toluidine (DMpT) and *o*-benzoic sulfimide (BS), the free radical initiator; cumene hydroperoxide (CHP), and the fluorophore; 2,5-bis(5′-butyl-2-benzoxazol-2-yl)thiophene (BBOT), as detailed in Table I. BBOT fluorophore is added for visual aid during the curing of this formulation.

### UV–vis spectroscopy

As expected from the aliphatic structure, distilled HEMA shows little absorption in UV spectra above 225 nm, while other additives show significant UV absorption as illustrated in Figure 1. For this reason, HEMA spectra are not shown in Figure 1. Table II summarizes the UV–vis spectroscopic results. The fluorophore, BBOT shows the absorption maxima at the longest wavelength of 371 nm with a much greater extinction coefficient of 48,723 in comparison to other additives.

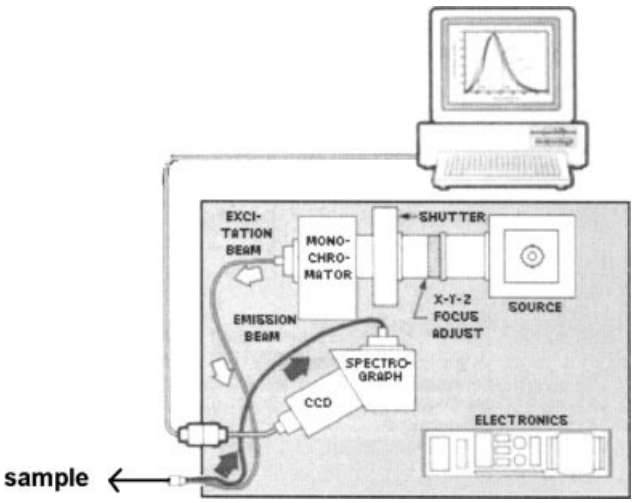


**Scheme 4** Set up of fluorescence spectrometer.

The application of UV–vis spectroscopy has shown that the absorption of the fluorophore is not affected by the presence of stabilizers, accelerators, and other common additives. This has been further verified by observing no changes in combined and simulated UV spectra of the mixtures. Therefore, we may conclude that nonreactive BBOT having an extinction coefficient which is much greater than the other ingredients will absorb energy at a wavelength that allows this molecule to be the main contributor to the fluorescence emission, if its fluorescence quantum yield is high enough.

### FTIR spectroscopy

#### Polymerization analysis of model formulation I

The IR method for this work is similar to that employed by McGettrick et al.[10] and forms the basis for comparing fluorescence spectroscopic techniques. Model formulations were polymerized by the method described above. Figure 2 shows the FTIR spectra of model formulation I during cure. It is noted that the terminal alkene peak at $\sim 810$ cm$^{-1}$ decreases sharply, while the internal standard peak at $\sim 1700$ cm$^{-1}$ due to carbonyl of ester changes to a smaller extent. Figure 3 shows monomer conversion to polymer by plotting the change in the C—H bending of the terminal carbon of the alkene relative to the carbonyl of the ester. It is noted in Figure 3 that the percent cure quickly rises to about 80% within 2 h of cure. This graph is the template that

**TABLE II**
**UV Absorption Maxima and Extinction Coefficients of Adhesive Formulation Additives**

| Ingredient | $\lambda_{max}$ | ε |
|---|---|---|
| BBOT | 371 | 48,723 |
| BS | 277 | 886 |
| CHP | 241 | 247 |
| DMpT | 306 | 1689 |

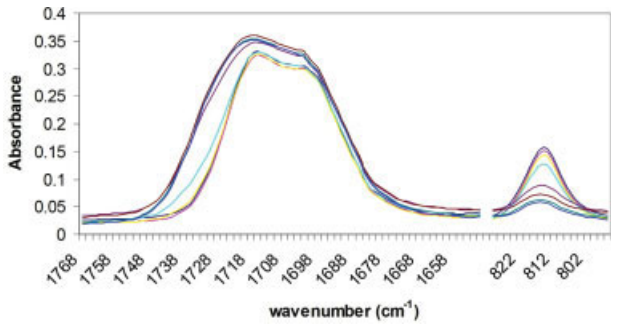


**Figure 2** FTIR spectra of model formulation I during polymerization. Cure time from top to bottom is 0.38, 0.95, 1.53, 2.10, 2.86, 3.63, and 4.58 h. [Color figure can be viewed in the online issue, which is available at www.interscience.wiley.com.]

we will compare with the results from fluorescence spectroscopy. It is also noted that the reaction for model formulation I only reaches ~ 80% conversion as a result of the polymerization at room temperature which is below the glass transition temperature of fully cured poly(HEMA) of about 60°C.[11] During polymerization, the glass transition temperature rises if cure temperature is above the maximum $T_g$.[12] The resin $T_g$ can be correlated to the conversion as demonstrated in epoxy. But DSC is not an *in situ* method.

## Polymerization analysis of model formulation II

Similar to model formulation I, another formulation was prepared to mimic a commercial anaerobic adhesive for use with off-the shelf products. Again, this is to establish a template for correlating the fluorescence cure monitoring. To this end, the product was prepared and cured with no additional purification. The composition of model formulation II is shown in Table III along with the chemical structures that have not been identified earlier in this article. A small amount of BBOT was added after making other ingredients total to be 100%. Among the ingredients in Scheme 5, propoxylated bisphenol A fumarate (PBPAF) is a soluble solid that is added to toughen the polymer. Polyethylene is used to reduce friction between the mating parts. Napthoquinone (NQ) and ethylene diamine tetra acetic acid tetra sodium salt (EDTA) are used to increase the shelf stability of the formulation. Since these additional ingredients are nonreactive, the reaction mechanism in formulation II is expected to be the same as formulation I where Scheme 1 represents the basic cure

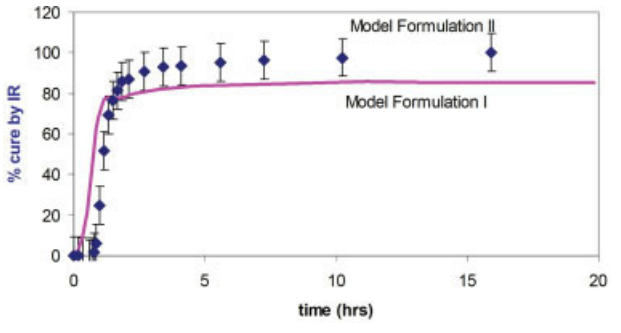


**Figure 3** Percent monomer conversion of model formulation I and II by IR method. [Color figure can be viewed in the online issue, which is available at www.interscience.wiley.com.]

**TABLE III**
**Composition of Model Formulation II**

| Ingredient | Weight % |
|---|---|
| TriEGMA | 68.98 |
| PBPAF | 25.00 |
| CHP | 1.00 |
| BS | 1.00 |
| DMpT | 1.00 |
| Poly(ethylene) | 2.00 |
| NQ | 0.01 |
| EDTA | 0.01 |
| Fumed silica | 1.00 |
| BBOT | 0.045 |

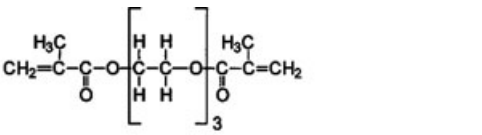

Triethylene glycol dimethacrylate (TriEGMA)

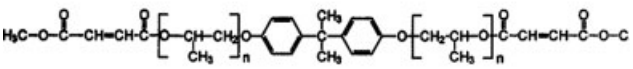

Propoxylated Bisphenol A fumarate (PBPAF)

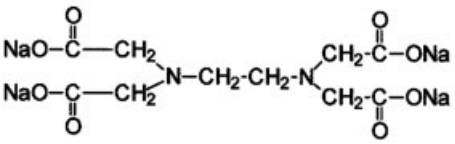

Ethylenediamine tetraacetic acid sodium salt (EDTA)

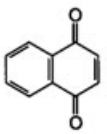

1, 4 – Naphthoquinone (NQ)

**Scheme 5** Chemical structures of the main ingredients for model anaerobic formulation II in addition to BS, DMpT, CHP.

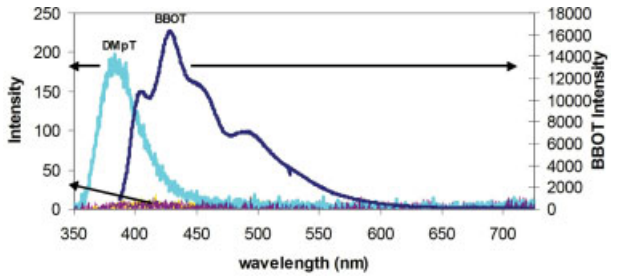


**Figure 4** Fluorescence emission of anaerobic formulation ingredients. Note that BBOT is on the secondary *y*-axis. CHP and BS show very weak fluorescence as indicated by the lowest spectra. [Color figure can be viewed in the online issue, which is available at www.interscience.wiley.com.]

mechanism. The extent of reaction of the monomer for model formulation II was calculated and plotted in Figure 3 together with model formulation I as a reference.

Cure monitoring results of model formulation I relative to model formulation II show that both behave similarly. As the cure time increases, both materials show a dramatic increase in monomer conversion before leveling off as the reaction slows to completion. Model formulation I shows a smaller induction time and reaches an ultimate cure extent of 80% in slightly more than 1 h. Because of the added stabilizers in model formulation II, the induction time is longer and polymerization is initially delayed by $\sim 0.75$ h. As a result, model formulation II reaches its ultimate cure state of $\sim 100\%$ cure in roughly 3 h. The glass transition temperature of model formulation II is 28.6°C which is lower than the $T_g$ of poly(HEMA). Therefore, model formulation II is able to achieve nearly 100% monomer conversion at room temperature. Additional stabilizer, NQ is necessary for commercial products to provide sufficient shelf life. It can be seen from these results that NQ does not reduce the overall cure speed greatly.

## Fluorescence spectroscopy

Before proceeding to fluorescence analysis of anaerobic formulations, it is important to point out the differences between the techniques with respect to cure monitoring. IR analysis is concerned specifically with the loss of monomer, or more specifically, the conversion of monomer to polymer. The process charts the change in the number of carbon–carbon double bonds and as a result, it is able to fairly accurately quantify the amount of monomer consumed. In contrast, fluorescence monitors the change in the microenvironment of the fluorophore. It is indirectly related to the polymerization process but is extremely sensitive to small changes in its immediate environment. The fluorophore that we are focusing on in this work, BBOT, is not expected to interact directly with the polymerization process. However, the change in the surroundings of this material is anticipated to cause a measurable change in its fluorescence.

### Analysis of monomer and stabilizer

A sample of HEMA was washed in 10% sodium hydroxide to remove the stabilizer and dried over calcium chloride. The monomer was then vacuum distilled and the collection flask was repeatedly changed until no fluorescence of the collected sample could be observed. The effect of the stabilizer 1,4-naphthoquinone, NQ on the fluorescence emission was then explored. Results indicate no significant fluorescence intensity of monomer either by itself or after adding NQ. This result is expected since quinones have little fluorescence due to the intersystem crossing to the triplet state.

### Analysis of other additives

The cure system ingredients BBOT, BS, DMpT, and CHP were each subjected to fluorescence emission scans using the UV absorption maxima identified in the UV–vis experiments as the excitation wavelength. The results of these scans for BBOT and DMpT are shown in Figure 4. Note that BBOT is shown on the secondary *y*-axis and gives an indication of its much greater ability to fluorescence relative to the other ingredients. The fluorescence of CHP and BS is much weaker than BBOT and DMpT, as barely visible on the primary axis. Based on absorbance measurements, it is possible to calculate a relative quantum yield for each additive, as tabulated in Table IV.

It is clear from this investigation that BBOT has at least a 40-fold increase in fluorescence capability in terms of relative quantum yield ($\Phi_{rel}$) as compared to DMpT, which shows the greatest $\Phi_{rel}$ among other additives. With respect to the measured emission intensity, BBOT is roughly 85 times stronger compared to all other cure ingredients because of its high extinction coefficient at the concentrations used in the anaerobic formulation.[13]

**TABLE IV**
**Relative Quantum Yields of Adhesive Formulation Additives**

| Ingredient | Φrel |
|---|---|
| BBOT | 800 |
| BS | 1 |
| CHP | 15 |
| DMpT | 20 |

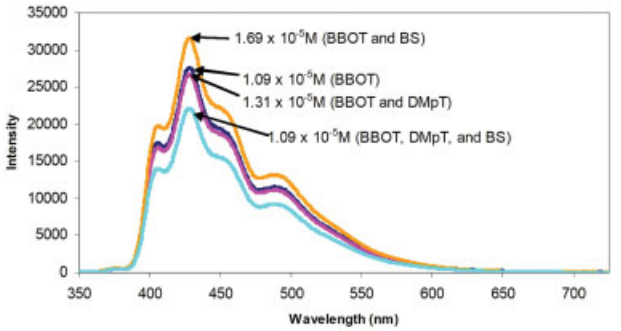


**Figure 5** Fluorescence spectra of anaerobic adhesive formulation additives. The concentration values shown are for BBOT. [Color figure can be viewed in the online issue, which is available at www.interscience.wiley.com.]

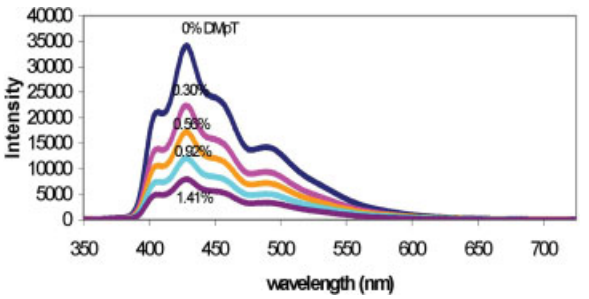


**Figure 6** Fluorescence spectra of BBOT ($5.35 \times 10^{-5}$ M) in ethyl acetate with increasing amounts of DMpT. [Color figure can be viewed in the online issue, which is available at www.interscience.wiley.com.]

The potential for raw material interaction was explored by analyzing the spectra for mixtures of BBOT, BS, and DMpT in the concentration ratios similar to the adhesive formulation, as outlined in Figure 5. The change in BBOT fluorescence intensity in Figure 5 gives the first indication that other additives, namely DMpT, may reduce BBOT fluorescence. The concentrations of BBOT have been added to the graph to illustrate this point. Generally, as the concentration of BBOT increases, the fluorescence intensity in this concentration range increases as well. To further support the observation that DMpT is responsible for this loss of intensity, the mixture of BBOT and BS appears to show no decrease in fluorescence intensity although the concentration of BBOT is indeed greater in this formulation. Calculating the ratio of the fluorescence intensity of BBOT divided by the respective concentration of BBOT helps to quantify these observations and the results are summarized in Table V. Two trends are readily apparent from this exercise. The first is that it appears that BS also participates in reducing the fluorescence emission of BBOT. Second, and perhaps more importantly, the fluorescence intensity ratio in the presence of DMpT is virtually identical regardless of the presence of BS leading to about 20% reduction in intensity. The results indicate that DMpT overrides any quenching caused by BS. The next step is to isolate the interaction of BBOT and DMpT.

The relationship between these two ingredients has been further explored to characterize the nature of this occurrence as well as to determine if it can be useful as a polymerization monitoring technique. Ethyl acetate was formulated with a fixed level of BBOT ($5.35 \times 10^{-5}$ M) and increasing amounts of DMpT. The fluorescence scans of these formulations in Figure 6 clearly indicate the quenching effect of DMpT concentration on BBOT fluorescence intensity.

Because we see no shift in the peak position of either the UV or fluorescence spectra, it is reasonable at this point to assume the phenomenon is the physical deactivation of the excited state of BBOT. Equation (1) describes the Stern–Volmer quenching equation.

$$\frac{F_0}{F} = 1 + k_q \tau_0 [\mathrm{Q}]$$

In this equation, $F_0$ and $F$ are the fluorescence intensities in the absence and presence of quencher, respectively. The term $k_q$ is the bimolecular quenching constant and $\tau_0$ is the fluorescence lifetime in the absence of quencher. These two terms are typically combined into one constant called the Stern–Volmer quenching constant $K_{SV}$. The term [Q] is the concentration of quencher, thus when the fluorescence intensity ratio is plotted against the concentration of quencher, straight line behavior is indicative of a single case of fluorophore and hence either static or dynamic quenching. Intuitively, the line has a $y$-intercept equal to one and $1/K_{SV}$ is the quencher concentration at which 50% of the fluorescence intensity is quenched. The data from the DMpT quenching of BBOT in ethyl acetate has been applied to Eq. (1) and plotted in Figure 7.

**TABLE V**
**Calculation of BBOT Fluorescence Intensity Ratios**

| Formulation no. | Fluorescence intensity ($I_f$) | BBOT concentration $C$ ($M \times 10^{-5}$) | $I_f/C$ | Other additives |
|---|---|---|---|---|
| 1 | 27,611 | 1.09 | 25,331 | None |
| 4 | 26,720 | 1.31 | 20,397 | DMpT |
| 5 | 31,582 | 1.69 | 18,688 | BS |
| 7 | 22,156 | 1.09 | 20,327 | DMpT + BS |

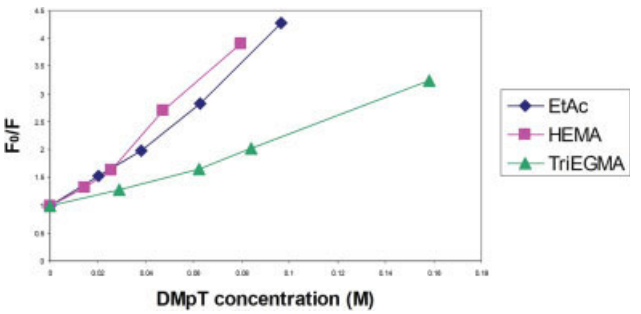


**Figure 7** Stern–Volmer plots of BBOT quenching by DMpT in ethyl acetate (Et Ac), HEMA and Tri EGMA. [Color figure can be viewed in the online issue, which is available at www.interscience.wiley.com.]

The straight line result indicates that we are seeing single mode quenching when these two ingredients are combined. Furthermore, by taking the reciprocal of the slope, we achieve 50% quenching at a concentration of 0.03*M* DMpT which translates to ~ 0.6% of the formulation. This is well in the range of the typical 1% value used in commercial adhesives. In addition to these calculations, it is also of interest to determine which mode of quenching is being observed.

With regard to mode, we are referring to static verses dynamic. As both types independently result in straight-line behavior with respect to Stern–Volmer plots, a method to evaluate the mechanism has been carried out. It is also important to recognize that a combination of both static and dynamic quenching results in deviation from the straight-line relationship. Because of this fact, we are therefore only looking at one specific type in this system.

As viscosity increases, molecular mobility and hence the potential for molecular collision decreases. Conversely, as temperature increases, molecular mobility increases resulting in increased potential for molecular collision. If no change in quenching is seen by either of these methods, the mode is static. If increased temperature increases quenching or increased viscosity reduces quenching, the mode is then dynamic. To this end, formulations containing fixed amounts of BBOT and increasing amounts of DMpT were prepared in HEMA and TriEGMA representing monomers with different base viscosities. The Stern–Volmer plots are shown below in Figure 7.

Two trends are readily apparent from these plots. The first is that both are straight lines indicating that only one type of quenching behavior is being observed. Second, and perhaps more importantly, the slope in more viscous TriEGMA case is much lower than that of HEMA or ethyl acetate. Therefore, we may conclude that the quenching mechanism is not only collisional, but also dynamic allowing us to represent the Stern–Volmer constant as $K_D$ which is more precise than the general form $K_{SV}$. The observation of a dynamic quenching mechanism should also prove to be a positive advantage for cure monitoring.

Taking this investigation one step further, the fluorescence lifetime ($\tau$) of BBOT is reported to be 1.2 ns,[14,15] in the absence of quencher. With this information, it is possible to calculate the bimolecular quenching constants ($K_q$) for each of the three systems above. The results are shown in Table VI. The values calculated for $K_q$ are in good agreement with diffusion controlled quenching reactions,[16] as is the case for the dynamic mechanism identified here. Higher values indicate some type of binding interaction while lower values can result from steric shielding of the fluorophore. The next step is to examine the effect of the physical environment on the fluorescence emission of BBOT.

The samples previously prepared to examine the effects of changing viscosity by UV-vis spectroscopy were examined here by fluorescence. The formulations containing a fixed amount of BBOT and increasing amounts of p(HEMA) dissolved in ethanol were scanned by fluorescence. The emission spectrum of each formulation was recorded and represents increasing viscosity as occurs during polymerization. The results show that viscosity does not appear to affect the fluorescence intensity of BBOT. Subsequently, the same formulations were re-examined with DMpT added to each formulation and shown in Figure 8(a).

In the presence of 1% DMpT, fluorescence intensity increases as the viscosity of the solution increases, presumably due to the reduced diffusion of the quencher DMpT in viscous solution.

All of the necessary information is now in place to apply the fluorescence technique to monitor the polymerization of anaerobic adhesives. By monitoring the change in fluorescence intensity during polymerization, it should be possible to correlate the collisional quenching of BBOT with monomer conversion. The intensity is expected to increase as polymerization proceeds due to reduced diffusion and quenching of DMpT as the viscosity of the polymerization medium increases.

## Polymerization analysis of model formulation I

The formulation was placed on a steel lap shear with a strip of tape as a spacer. A quartz disc was

**TABLE VI**
**Bimolecular Quenching Constants**

| Solvent/monomer | $K_D$ ($M^{-1}$) | $K_q$ ($M^{-1}$ $s^{-1}$) |
|---|---|---|
| Ethyl acetate | 33.79 | $2.80 \times 10^{10}$ |
| HEMA | 37.99 | $3.17 \times 10^{10}$ |
| TriEGMA | 14.34 | $1.20 \times 10^{10}$ |

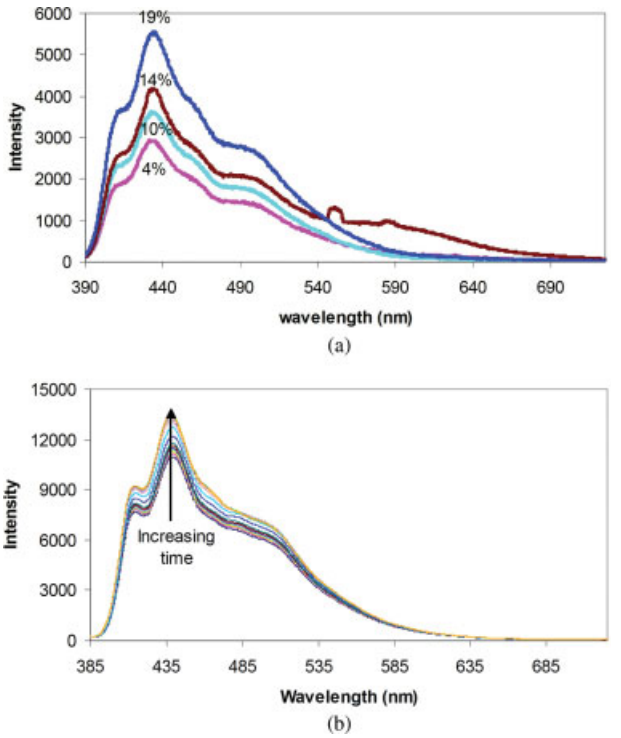


**Figure 8** (a) Fluorescence spectra of BBOT ($5.35 \times 10^{-5}$ M) in ethanol in the presence of 1% DMpT. The values shown indicate the weight percent of p(HEMA) present in the formulation. (b) Fluorescence spectra of BBOT in model formulation I during anaerobic polymerization. 0.15, 0.39, 0.54, 0.78, 0.93, 1.51, 2.22, 2.75, 3.50, 3.99, 4.01, 5.00, 5.50, and 5.86 h from bottom to top. [Color figure can be viewed in the online issue, which is available at www.interscience.wiley.com.]

clamped to the lap shear providing both a uniform gap and an anaerobic environment. A schematic of this sampling method is shown in Scheme 3. Sample spectra were recorded every minute until the reaction reached a plateau. Several spectra are shown in Figure 8(b) to illustrate the change in intensity observed during the polymerization process. As predicted, the fluorescence intensity did in fact increase as polymerization proceeded. It is also evident that no peak shift occurred during the polymerization process as was also expected from the previous section.

Figure 9(a) shows the changes in the fluorescence intensity with cure time. This figure also displays the results from the FTIR cure monitoring study. As can be seen, they both proceed in a very similar manner. The results show that the process of monitoring the fluorescence quenching of BBOT during polymerization can be used to follow the reaction progress.

### Polymerization of model formulation II

This technique was then applied to model formulation II to determine the efficacy of fluorescence cure monitoring in a fully formulated adhesive composition. The formulation was cured as described earlier and the results of the fluorescence scans and intensity changes show a trend similar to model formulation I in that a sharp increase in intensity is observed early in the reaction process followed by a leveling off as the reactions slows. The primary difference here again is that an initial induction period occurs prior to polymerization due to the added stabilizers. Figure 9(b) compares favorably the fluorescence results with IR results. Thus both model formulations show the same effect of fluorescence quenching of BBOT as a result of the diffusion of DMpT. The final result here is that fluorescence cure monitoring of commercial anaerobic adhesives is a viable process and provides greater diversity and sensitivity than is typical of IR techniques which are limited by their inherent accuracy and the difficulty to employ fiber-optic techniques.

## CONCLUSIONS

Since the monomer HEMA is nonfluorescent, fluorescence spectroscopy has shown that the fluorophore, BBOT is most intense in comparison to other ingredients and can be quenched by an amine accelerator, DMpT. The relative quantum yields of the

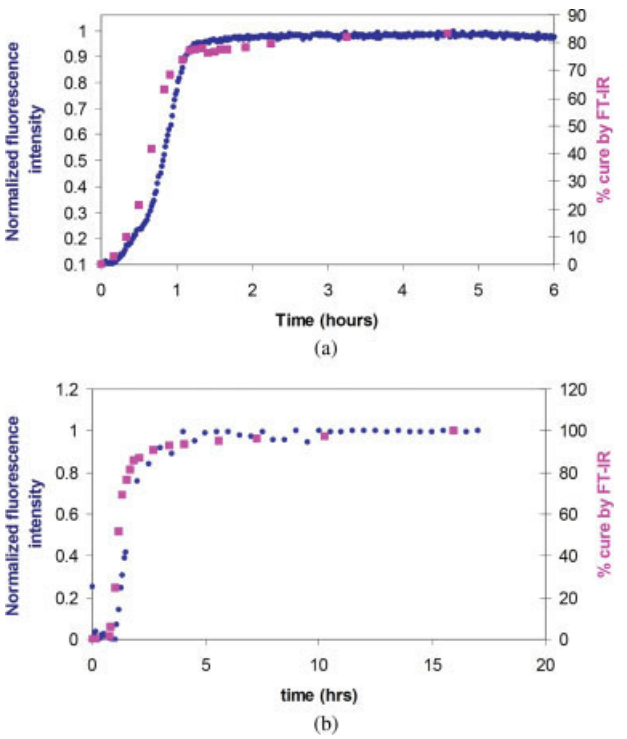


**Figure 9** (a) Comparison of cure monitoring techniques of model formulation I. (●: fluorescence intensity, ■: IR results). (b) Comparison of cure monitoring techniques of model formulation II. [Color figure can be viewed in the online issue, which is available at www.interscience.wiley.com.]

formulation ingredients show BBOT as the dominant fluorescence emitter as compared to other additives. As viscosity increases, the amount of fluorescence quenching decreases due to reduced diffusion of DMpT, as demonstrated in ethanol solution by adding successively increasing amounts of poly(HEMA). During polymerization, the fluorescence intensity of BBOT increases due to reduced collisional quenching by DMpT. The single mode collisional quenching phenomenon has been confirmed by constructing Stern–Volmer plots.

Thus by monitoring the fluorescence intensity relative to cure time, as illustrated by the fiber-optic instrument such as in Scheme 4 it is possible to use fluorescence spectroscopy to follow anaerobic polymerization.[15] Fluorescence results show excellent correlation with FTIR techniques.

## References


1. Hill, L.W. In Proceedings of the 69th Annual Meeting of the Federation for Coatings Technology; 1992; Vol. 64, p 808.
2. Haviland, G. S. Machinery Adhesives for Locking and Sealing; Marcel Dekker: New York, 1986.
3. Yang, D. B. Appl Spectrosc 1993, 47, 1425.
4. Beaunez, P.; Helary, G.; Sauvet, G. J Polym Sci Part A: Polym Chem 1994, 32, 1459.
5. Wellman, S.; Brockmann, H. Int J of Adhes Adhes 1994, 14, 47.
6. Moane, S.; Raftery, D. P.; Smyth, M. R.; Leonard, R. G. Int J Adhes Adhes 1999, 19, 49.
7. Rich, R. D. Handbook of Adhesive Technology; Marcel Dekker: New York, 1994.
8. Dang, W. B.; Sung, N. H. Polym Eng Sci 1994, 34, 707.
9. Paik, H. J.; Hestermann, D. K.; Sung, N. H. SPE ANTEC 1995, 41, 2816.
10. McGettrick, B. P.; Vij, J. K.; McArdle, C. B. J Appl Polym Sci 1994, 52, 737.
11. Shen, M. C.; Strong, J. D.; Matusik, F. J. J Macromol Sci Phys 1967, 1, 15.
12. Enns, J. B.; Gillham, J. K. In Polymer Characterization; Craver, C. D., Ed.; American Chemical Society: Washington, DC, 1983; p 27. Advances in Chemistry Series 203.
13. Maandi, E. Ph.D. Thesis, University of Connecticut, 2001.
14. Asetti, F.; Elisei, F.; Mazzucato, U. J Luminescence 1996, 68, 15.
15. Peckan, O.; Yilmax, Y.; Okay, O. J Appl Polym Sci 1996, 61, 2279.
16. Lakowicz, J. R. Principles of Fluorescence Spectroscopy, 2nd ed.; Kluwer Academic/Plenum: New York, 1999; p 241.